Estimation of spontaneous neuronal activity using homomorphic filtering

Sukesh Kumar Das[1][0000−0002−6303−0800], Anil K. Sao[2][0000−0001−5316−5528], and Bharat Biswal[3][0000−0002−3710−3500]

[1] Indian Institute of Technology Mandi, HP 175005, India
d17025@students.iitmandi.ac.in
[2] Indian Institute of Technology Mandi, HP 175005, India
anil@iitmandi.ac.in
[3] New Jersey Institute of Technology, Newark, NJ 07102, USA
bharat.biswal@njit.edu

Abstract. Blood Oxygen Level-Dependent (BOLD) signal changes in functional magnetic resonance imaging (fMRI) measures neuronal activities blurred by hemodynamic response function (HRF) and hence may not be reliable to estimate functional connectivity (FC). Several methods have been attempted to estimate the neuronal activity signal (NAS) from the observed BOLD signal. Using this as a blind source separation problem, these methods assume a parametric model of HRF. But it is not clear if these models accurately reflect the biophysical process. In this paper, we have proposed an approach based on a homomorphic filter (HMF) to deconvolve NAS from resting state fMRI (rs-fMRI) time course. It exploits the hypothesis that the HRF has predominantly low frequency energy in comparison to the NAS. Hence, by choosing an appropriate value of cutoff quefrency with the help of thresholded BOLD signal after HMF, HRF can be suppressed from observed BOLD signal to get an estimate of NAS. The estimated NAS, in the framework of dictionary learning (DL), is able to produce subtle resting state networks (RSNs) in comparison with the existing blind deconvolution (BD) method. The Jaccard similarity distance between RSNs by taking random samples and the entire subjects underpins the robustness of the estimated RSNs. Another quantitative comparison has also been drawn to show the efficacy of the HMF in the estimation of NAS using the maximum normalized cross-correlation coefficient (MNCC) distribution for different RSNs.

Keywords: Deconvolution · Homomorphic filtering · rs-fMRI · RSNs.

1 Introduction

Blood oxygen level-dependent (BOLD) signal acquired during functional magnetic resonance imaging (fMRI), attempts to measure the neuronal activity in the human brain. Studying spontaneous brain activity without any stimulus has emerged in an alternative way to study the brain function [2]. Functional connectivities (FC), computed using the observed BOLD time course, over the different

spatial regions, without any explicit stimulus are called resting state networks (RSNs). The neuronal activity, observed in the BOLD signal, is modulated by hemodynamic response function (HRF) and mathematically expressed as [8]

$$m_o[n] = s[n] * h[n] + \epsilon[n], \tag{1}$$

where, $s[n]$ is the underlying neuronal activity signal (NAS) that carries timing information of neuronal events, $h[n]$ is the HRF which models the dynamic changes in the blood flow and $\epsilon[n]$ is the noise evoked in measurement. As the HRF blurs the NAS and varies across the voxels, its effect should be removed from the BOLD signal to estimate the FC resulted due to NAS. Several methods have been proposed to estimate $s[n]$ from the observed $m_o[n]$ [3, 13, 23], so that RSNs can be estimated efficiently. The estimation of $s[n]$ from $m_o[n]$ is challenging in rs-fMRI because it is void of the experimental paradigm [23]. The NAS can be estimated from rs-fMRI using a parametric blind deconvolution approach with the help of spontaneous pseudo-events [23]. Here, HRF is estimated as a weighted combination of three bases at minimum noise variance and then Wiener filter deconvolves the spontaneous neuronal activity. Karahanouglu and colleagues introduced total activation to estimate activity related signals by imposing data fitting and spatio-temporal regularizations [13]. Later, the activity related signal is used in inverse differential hemodynamic operator [7] and activity signal is obtained for the rest and task conditions. A joint estimation of the HRF and NAS is carried out by solving a semi-blind deconvolution problem with the constraint that the derivative of NAS is sparse [3]. All of the deconvolution methods assume either a parametric model of the HRF or uniformity of HRF across the brain regions and also limited due to the presence of noise (physiological and head movement). The ambiguity in the case of parametric model of HRF is that the optimal number of parameters is still unclear to represent the actual bio-physical process [20] and intra and inter-subject variability of HRF is also a serious concern in the deconvolution of NAS from rs-fMRI [5].

In this paper, we have proposed an approach, to estimate NAS from m_o, which does not assume any parametric model of HRF. It is based on the observation that the HRF is relatively slow varying in nature and can be associated with low frequency range of spectrum of BOLD signal. This observation may suggest to use a high pass filter (HPF) to suppress the effect of HRF in observed BOLD signal and the resultant BOLD signal will have mostly the information of NAS. However, a simple HPF cannot be used to separate both HRF and NAS, as they are multiplicative in nature in the frequency domain. The proposed method is based on homomorphic filtering (HMF) to estimate NAS from the BOLD rs-fMRI data. In this filtering, the observed BOLD time course is transformed into cepstrum domain, where HRF and NAS are additive in nature. The separation of them in cepstrum domain is done by high pass liftering (HPL) with an optimal value of cutoff quefrency (Q_c). The Q_c is obtained by maximizing the value of a metric, normalized cross correlation coefficients (NCC) between estimated NAS and thresholded rs-fMRI BOLD time course (we call it probable neuronal

variable (PNV)). The resultant NAS is employed in the framework of online dictionary learning (ODL) to estimate RSNs [17, 18]. It should be noted that the HMF was studied for task fMRI [20], where the knowledge of experimental design aids in the estimation of NAS. For task related fMRI, it is assumed that the NAS is resulted due to the similar external stimuli. So, the NAS is not much variant across the subjects, especially for a particular brain region associated with the task. On the other hand, the rs-fMRI hasn't such direct advantage and hence, NAS is assumed to be more variant as activations occur due to intrinsic stimuli. Therefore, there is a need to estimate voxel-wise NAS for the subtle RSNs.

The organization of the paper is as follows: Section 2 explains the proposed method including estimation of NAS and RSNs using DL method. Section 3 describes the data and tools used in the method. Experimental results are explained in Section 4 and the discussion is provided in Section 5.

2 Method

Schematic diagram for the estimation of the RSNs using the proposed method, has been illustrated in Fig. 1. Here, the preprocessed BOLD signal is empirically decomposed (EMD) and the first three intrinsic mode functions (IMFs) are considered in HMF to suppress the drift [1, 10]. The lower oscillatory modes (forth and onwards) can be associated with drift component present in BOLD signal. The NAS is then estimated for every individual voxel using homomorphic deconvolution of the obtained signal and is used to form a time-voxel matrix. Finally, the matrix is decomposed using ODL to estimate RSNs. The Homomorphic de-

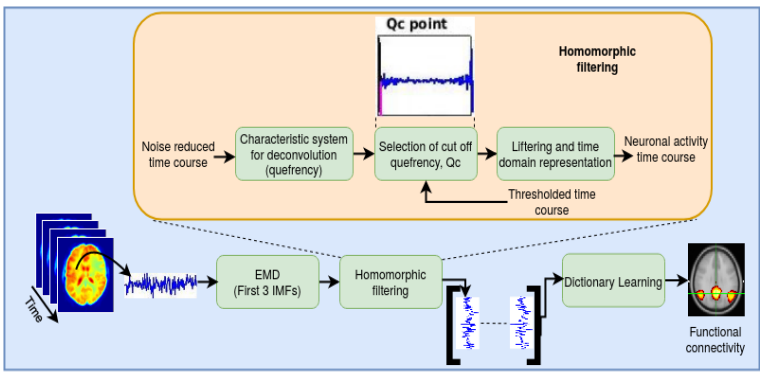

Fig. 1: Block diagram for estimation of RSNs using NAS obtained by HMF

convolution is performed on the noise suppress signal with the idea that the

HMF converts convolution of two time domain signals into a linear sum of them in the cepstrum domain [19]. Following that, if two signals have characteristics of energy concentrated in different ranges of frequencies, the separation of the same can be relatively easier in the cepstrum domain. As the HRF has energy concentrated mostly in low frequency (in comparison to NAS) because of its slowly varying nature. Thus, separation of the NAS and HRF can be relatively easier using HMF. The noise reduced BOLD signal can be written as

$$m_d[n] = s[n] * h[n], \tag{2}$$

In the frequency domain, it can be written as

$$M_d(e^{j\omega}) = S(e^{j\omega})H(e^{j\omega}), \tag{3}$$

where, $M_d(e^{j\omega})$, $S(e^{j\omega})$ and $H(e^{j\omega})$ are the Fourier transform (FT) of $m_d[n]$, $s[n]$ and $h[n]$ respectivelly. In Cepstrum domain, m_d can lead to be

$$\tilde{m}_d[n] = F^{-1}\{\log M_d(e^{j\omega})\} = F^{-1}\{logS(e^{j\omega})\} + F^{-1}\{logH(e^{j\omega})\} = \tilde{s}[n] + \tilde{h}[n], \tag{4}$$

Now, the $\tilde{m}_d[n]$ is represented as a linear sum of NAS and HRF in the cepstrum domain. Thus, after HPL using a suitable Q_c, NAS can be separated in cepstrum domain. Now, estimated NAS in cepstrum domain,

$$\hat{\tilde{s}}[n] = HPL\{\tilde{m}_d[n]\}, \tag{5}$$

Time domain representation of the estimated NAS is obtained by inverse FT of exponential of the FT of the liftered cepstrum, therefore

$$\hat{s}[n] = F^{-1}\{e^{F\{\hat{\tilde{s}}[n]\}}\} \tag{6}$$

2.1 Selection of the cut off quefrency

Selection of a suitable Q_c to estimate $\hat{s}[n]$ from the observed $m_o[n]$ in rs-fMRI is challenging, because if we choose a very small value of Q_c then, the resultant signal will have the effect of HRF, which is undesirable. On the other hand, the estimated $\hat{s}[n]$ may not represent the complete NAS for a large value of the Q_c. Hence, to obtain an optimal value of Q_c, we have followed a data driven approach. We have varied the length of DFT (discrete approximation of Fourier transform) and Q_c and for each choice of a pair (DFT length and Qc), normalized cross correlation coefficient (NCC) is computed between NAS ($\hat{s}[n]$) and PNV ($s_p[n]$). The PNV is based on the hypothesis that rs-fMRI is spontaneous event related and the events are mostly captured by choosing the locations, in the BOLD time course, which crosses a predefined threshold value [6, 16, 21]. The maximum NCC is given as

$$MNCC = \underset{\hat{s}[n]}{\text{argmax}} \frac{max\{|r_{\hat{s}s_p}|\}}{\sqrt{\sum_{n=1}^{a} \hat{s}[n]^2}\sqrt{\sum_{n=1}^{b} s_p[n]^2}} \tag{7}$$

where a and b are the signal lengths of $\hat{s}[n]$ and $s_p[n]$ respectively and $r_{\hat{s}s_p}$ is the cross correlation of the signals, $\hat{s}[n]$ and $s_p[n]$.

2.2 Connectivity maps using online dictionary learning (ODL)

The DL exploits the sparse behavior of the RSNs over an over-complete dictionary [4,11,14,18]. It decomposes multi-subject rs-fMRI data (time-voxel matrix) to produce spatial maps (RSNs). The NAS, $\mathbf{S} \in \mathbb{R}^{nm \times v}$ is decomposed as

$$\mathbf{S} \approx \mathbf{DA} \quad with \quad \mathbf{D} \in \mathbb{R}^{nm \times k} \quad and \quad \mathbf{A} \in \mathbb{R}^{k \times v} \ . \tag{8}$$

The $\mathbf{S}$ is obtained by temporally concatenating n number of consecutive NAS volumes obtained from m number of subjects each with v number of voxels. $\mathbf{D}$ consists k dense temporal atoms (every column) and the coefficient matrix, $\mathbf{A}$ consists k sparse spatial maps (every row). The atoms or basis vectors in $\mathbf{D}$ learned such that the rows ($\mathbf{a}_i$) of the matrix $\mathbf{A}$ corresponds to k number of RSNs. For the decomposition, sparsity inducing penalty is combined with the data fitting term and it leads to the following optimization problem:

$$\underset{\mathbf{D},\mathbf{A}}{\operatorname{argmin}} \|\mathbf{S} - \mathbf{DA}\|_F^2 \ + \lambda \| \ \mathbf{A}^T \|_{\mathbf{1}} \ \textbf{s.t.} \ \forall j, \|\mathbf{D}_j\|_2 \ \leq 1. \tag{9}$$

This equation is solved using ODL [17]. Further, all time points, in a time course at subject level, are mapped to low rank (p) subspace and final rank k decomposition is performed over concatenated data. The decomposition of the data with suitable initialization of atoms extracts reliable RSNs [9, 18]. The optimization problem (Eq. 9) with respect to the $\mathbf{D}$ and the $\mathbf{A}$ is not jointly convex and is solved by minimizing over one while keeping the other one fixed.

3 Data description and tools

The experiments for the proposed method are carried out using rs-fMRI data taken from UCLA consortium for Neuropsychiatric phenomics data set [4]. A total of 40 healthy participants (age = 21 − 50, 18F, 22M) are considered in this study. The data were acquired on a 3T Siemens Trio scanner. The fMRI data were acquired using the following scan parameters: TR (repetition time) = 2,000ms; TE (echo time) = 29 ms; field of view = 192mm ; flip angle = 72°; # slices (axial) = 34; slice thickness = 4mm with gap = 0; matrix size = 64×64; #images = 152. The data were pre-processed using SPM12 [5] with MATLAB R2019a. The initial 4 time points across subjects were discarded to get a steady magnetization. Anatomical images were reoriented w.r.t. the Montreal Neurological Institute (MNI) space and functional images were reoriented w.r.t. the anatomical images. Functional images were realigned followed by slice time correction. Anatomical images were co-registered to functional images and it was segmented into gray matter (GM), white matter (WM) and cerebro-spinal fluid (CSF). Functional images were then normalized to MNI space using the deformation field obtained in segmentation. The normalized functional images were smoothed with a Gaussian kernel of FWHM $5mm \times 5mm \times 5mm$. The time courses are band passed to reduce the high frequency physiological noise.

[4] https://openneuro.org/datasets/ds000030/versions/00016

[5] http://www.fil.ion.ucl.ac.uk/spm/

4 Experimental results

The output of the steps involved in estimation of NAS using HMF has been demonstrated in Fig. 2. A voxel time course ($m[n]$), taken from the left lateral parietal cortex (lLPC; MNI coordinate: $-48, 62, 34$) of default mode network (DMN) is represented in Fig. 2(a). The drift is then subtracted and transformed into cepstrum domain using HMF. The Q_c, for the time course is 3 at DFT length of 158. In cepstrum, the right part of the Q_c is considered as the NAS and the left part of the Q_c can be associated with the HRF. Time domain reconstruction of HRF and NAS are shown in Figs. 2(b) and (c) respectively. The PNV (blue) is obtained by thresholding (threshold value=1) the standardized noise suppressed time course, $m_d[n]$. For the given signal, computed MNCC is 0.544 ($p < 0.05$).

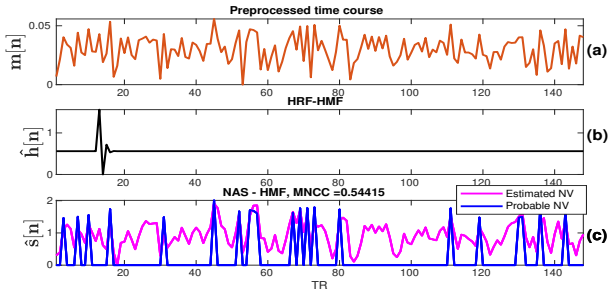

Fig. 2: Deconvolution using HMF:(a) preprocessed time course from the lLPC, (b) reconstructed signal related to HRF and (c) estimated NAS superimposed with PNV

4.1 Connectivity maps during rest using estimated NAS

The RSNs are estimated for the healthy control in rest and obtained using pre-processed BOLD time course and estimated NAS by BD and HMF methods with the ODL optimization Eq. 9. The reduced dimensions (p) used in the experiment is same as the value of the $k(= 28)$ and the values of the sparsity controlling parameter (λ) is 10. The six exemplary RSNs (anterior DMN - aDMN, medial sensory motor network - MSMN, auditory network - Aud, posterior DMN - pDMN, dorsal attention network - DAN and superior visual network - SVN) have been illustrated in Fig. 3. We could identify corresponding regions associated with each of the RSNs using NAS obtained by HMF. For example, in aDMN, we could identify the medial pre-frontal cortex, anterior cingulate and inferior parietal region. Similarly, the auditory network includes the Heschl gyrus, primary and associative auditory cortices, superior temporal, and insular cortices. Here, all six networks appear well by preserving the symmetricity in the case of NAS estimated by HMF. The RSNs show good localization with less spurious than the maps obtained by pre-processed and blind deconvolved (BD) time course.

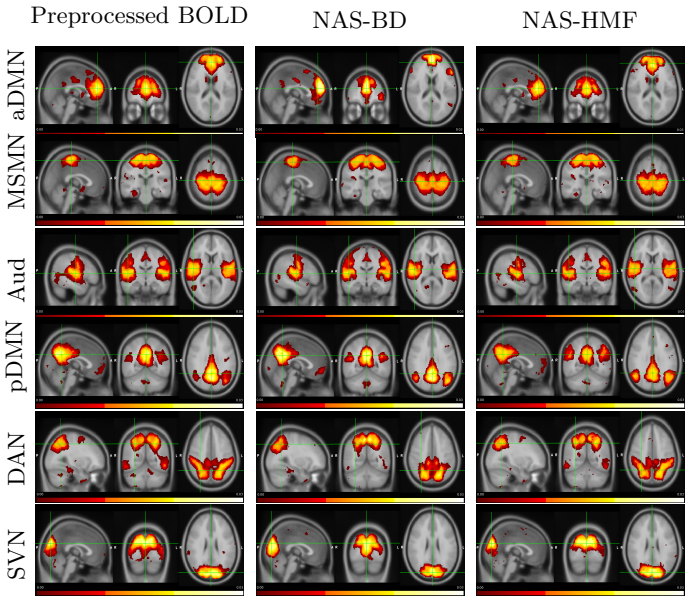

Fig. 3: Sagital, coronal and axial views of RSNs (from top: aDMN, MSMN, Aud, pDMN, DAN and SVN) obtained with ODL using conventionally preprocessed BOLD, NAS using BD and HMF respectively. All RSNs are presented in same scale$(0 - 0.3)$

4.2 Robustness of the RSNs

For the lack of the ground truth, the robustness of the estimated RSNs is demonstrated using two quantitative metric namely Jaccard similarity distances (JSD) and MNCC. We have used two sub-sampling schemes while using ODL and the decomposition was repeated for 25 times to obtain RSNs. In each repetition, out of 40 subjects, 20 subjects and 30 subjects are taken as a random subset and voxel-wise NAS is estimated using BD and HMF. The six RSNs (aDMN, MSMN, Aud, pDMN, DAN and SVN) are identified manually for every repetition of the two methods. A total of 150 RSNs is obtained using each of the two methods with one of the sub-sampling schemes. Each of these RSNs obtained with random subsample is compared with the respective RSNs obtained with 40 subjects (Fig. 3) using JSD [12]. The similarity distances with the two subsample schemes (row wise) for the two methods have been presented in Figs. 4(a) and 4(b) respectively. The average of the similarity scores of 150 RSNs with 20 random subjects for the BD method and the HMF methods are 0.57 ± 0.16 and 0.66 ± 0.09 respectively. For the 30 random subjects, the average similarity scores are 0.61 ± 0.17 and 0.74 ± 0.09 for the two methods respectively.We have also computed the MNCC between PNV and estimated NAS. The time courses were extracted from the six RSNs obtained using the proposed approach and MNCCs were computed for both proposed and BD approaches for 40 healthy control subjects. The mean of the MNCC for BD and HMF methods for the

given six RSNs are (0.201, 0.261), (0.198, 0.258), (0.201, 0.266), (0.198, 0.259), (0.202, 0.274) and (0.203, 0.256) respectively.

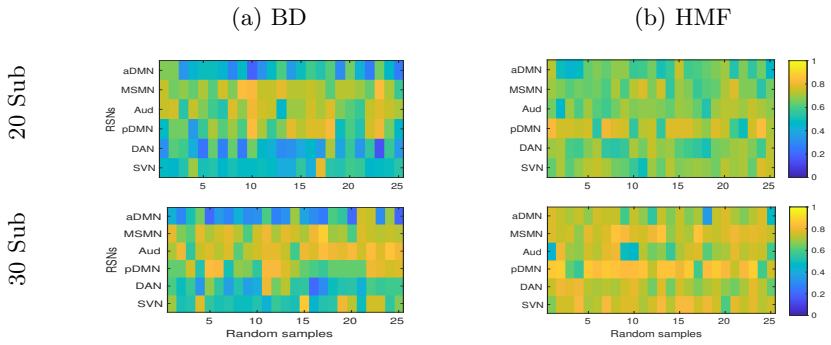

Fig. 4: JSD of RSNs between random 20 subject FCs (first row) and 30 subject FCs (second column) for BD (Fig. 4(a)) and HMF (Fig. 4(b)) deconvolution.

5 Discussion

In HMF, the BOLD time courses can be represented as a linear sum of HRF and NAS in the cepstrum domain. By choosing a suitable Q_c, NAS and HRF are separated. The separation was relatively easier because of the low frequency characteristic of the HRF and it is achieved with a hypothesis driven PNV which is used to maximize the NCC. The mean of the MNCC demonstrates the statistical significance of NAS in comparison with the BD for the predominant RSNs ($\rho < 0.05$).

It has been demonstrated that the estimated NAS can produce RSNs with fair spatial localization and symmetricity in the ODL framework. The method is more effective in removing spurious voxels than the traditional BOLD or BD method (see Fig. 3). The RSNs estimated using HMF demonstrates that the average similarity with the entire subjects increases with the increased number of random subjects which is expected but there is not much difference in variance for every case(see Fig. 4). The mean and the standard deviation of the JSD underpins that the reliability of the RSNs, obtained using the proposed method is more than that of BD approach. The reliability for the aDMN and DAN are very less in the case of BD method even if the size of the random sample is increased. Moreover, the work does not require the optimal number of parameters which can accurately model the HRF. As HRF is variant across the brain and subject, parametric model may not be a reliable choice in deconvolution whereas the proposed method estimates voxel wise NAS across the brain without necessitating any parametric assumption of HRF. We have kept selection of the Q_c as data driven procedure with the help of point process analysis [15, 16, 21, 22]. In the future, we will demonstrate our work in different pathological conditions.

References

1. Aggarwal, P., Gupta, A., Garg, A.: Joint estimation of hemodynamic response function and voxel activation in functional MRI data. In: International Conference on Medical Image Computing and Computer-Assisted Intervention. pp. 142–149. Springer (2015)
2. Bijsterbosch, J., Smith, S.M., Beckmann, C.F.: Introduction to resting state fMRI functional connectivity. Oxford University Press (2017)
3. Cherkaoui, H., Moreau, T., Halimi, A., Ciuciu, P.: Sparsity-based blind deconvolution of neural activation signal in fMRI. In: IEEE International Conference on Acoustics, Speech and Signal Processing (ICASSP). pp. 1323–1327. IEEE (2019)
4. Das, S.K., Sao, A.K.., Biswal, B.: Precise estimation of resting state functional connectivity using empirical mode decomposition. In: International Conference on Brain Informatics. pp. 75–84. Springer (2020)
5. Deshpande, G., Sathian, K., Hu, X.: Effect of hemodynamic variability on granger causality analysis of fMRI. Neuroimage **52**(3), 884–896 (2010)
6. Esfahlani, F.Z., Jo, Y., Faskowitz, J., Byrge, L., Kennedy, D., Sporns, O., Betzel, R.: High-amplitude co-fluctuations in cortical activity drive functional connectivity. bioRxiv p. 800045 (2020)
7. Friston, K.J., Mechelli, A., Turner, R., Price, C.J.: Nonlinear responses in fMRI: the balloon model, volterra kernels, and other hemodynamics. NeuroImage **12**(4), 466–477 (2000)
8. Glover, G.H.: Deconvolution of impulse response in event-related bold fMRI. Neuroimage **9**(4), 416–429 (1999)
9. Halko, N., Martinsson, P.G., Tropp, J.A.: Finding structure with randomness: Probabilistic algorithms for constructing approximate matrix decompositions. SIAM review **53**(2), 217–288 (2011)
10. Huang, N.E., Shen, Z., Long, S.R., Wu, M.C., Shih, H.H., Zheng, Q., Yen, N.C., Tung, C.C., Liu, H.H.: The empirical mode decomposition and the hilbert spectrum for nonlinear and non-stationary time series analysis. Proceedings of the Royal Society of London. Series A: mathematical, physical and engineering sciences **454**(1971), 903–995 (1998)
11. Iqbal, A., Seghouane, A.K.: Dictionary learning algorithm for multi-subject fMRI analysis via temporal and spatial concatenation. In: Proceedings of International Conference on Acoustics, Speech and Signal Processing (ICASSP). pp. 2751–2755. IEEE (2018)
12. Jaccard, P.: The distribution of the flora in the alpine zone. 1. New phytologist **11**(2), 37–50 (1912)
13. Karahanoğlu, F.I., Caballero-Gaudes, C., Lazeyras, F., Van De Ville, D.: Total activation: fMRI deconvolution through spatio-temporal regularization. Neuroimage **73**, 121–134 (2013)
14. Lee, K., Tak, S., Ye, J.C.: A data-driven sparse GLM for fMRI analysis using sparse dictionary learning with MDL criterion. IEEE Transactions on Medical Imaging **30**(5), 1076–1089 (2010)
15. Li, W., Li, Y., Hu, C., Chen, X., Dai, H.: Point process analysis in brain networks of patients with diabetes. Neurocomputing **145**, 182–189 (2014)
16. Liu, X., Duyn, J.H.: Time-varying functional network information extracted from brief instances of spontaneous brain activity. Proceedings of the National Academy of Sciences **110**(11), 4392–4397 (2013)

17. Mairal, J., Bach, F., Ponce, J., Sapiro, G.: Online learning for matrix factorization and sparse coding. Journal of Machine Learning Research **11**(1) (2010)
18. Mensch, A., Varoquaux, G., Thirion, B.: Compressed online dictionary learning for fast resting-state fMRI decomposition. In: Proceedings of 13th International Symposium on Biomedical Imaging (ISBI). pp. 1282–1285. IEEE (2016)
19. Oppenheim, A., Schafer, R.: Homomorphic analysis of speech. IEEE Transactions on Audio and Electroacoustics **16**(2), 221–226 (1968)
20. Sreenivasan, K.R., Havlicek, M., Deshpande, G.: Nonparametric hemodynamic deconvolution of fMRI using homomorphic filtering. IEEE transactions on medical imaging **34**(5), 1155–1163 (2014)
21. Tagliazucchi, E., Balenzuela, P., Fraiman, D., Chialvo, D.R.: Criticality in large-scale brain fMRI dynamics unveiled by a novel point process analysis. Frontiers in physiology **3**, 15 (2012)
22. Tagliazucchi, E., Siniatchkin, M., Laufs, H., Chialvo, D.R.: The voxel-wise functional connectome can be efficiently derived from co-activations in a sparse spatio-temporal point-process. Frontiers in neuroscience **10**, 381 (2016)
23. Wu, G.R., Liao, W., Stramaglia, S., Ding, J.R., Chen, H., Marinazzo, D.: A blind deconvolution approach to recover effective connectivity brain networks from resting state fMRI data. Medical image analysis **17**(3), 365–374 (2013)